Characteristics and Impacts of Extratropical Rossby Wave Breaking during the Atlantic Hurricane Season

GAN ZHANG AND ZHUO WANG

Department of Atmospheric Sciences, University of Illinois at Urbana–Champaign, Urbana, Illinois

MELINDA S. PENG

Naval Research Laboratory, Monterey, California

GUDRUN MAGNUSDOTTIR

Department of Earth System Science, University of California, Irvine, Irvine, California

(Manuscript received 4 June 2016, in final form 12 December 2016)

ABSTRACT

This study investigates the characteristics of extratropical Rossby wave breaking (RWB) during the Atlantic hurricane season and its impacts on Atlantic tropical cyclone (TC) activity. It was found that RWB perturbs the wind and moisture fields throughout the troposphere in the vicinity of a breaking wave. When RWB occurs more frequently over the North Atlantic, the Atlantic main development region (MDR) is subject to stronger vertical wind shear and reduced tropospheric moisture; the basinwide TC counts are reduced, and TCs are generally less intense, have a shorter lifetime, and are less likely to make landfalls. A significant negative correlation was found between Atlantic TC activity and RWB occurrence during 1979–2013. The correlation is comparable to that with the MDR SST index and stronger than that with the Niño-3.4 index. Further analyses suggest that the variability of RWB occurrence in the western Atlantic is largely independent of that in the eastern Atlantic. The RWB occurrence in the western basin is more closely tied to the environmental variability of the tropical North Atlantic and is more likely to hinder TC intensification or reduce the TC lifetime because of its proximity to the central portion of TC tracks. Consequently, the basinwide TC counts and the accumulated cyclone energy have a strong correlation with western-basin RWB occurrence but only a moderate correlation with eastern-basin RWB occurrence. The results highlight the extratropical impacts on Atlantic TC activity and regional climate via RWB and provide new insights into the variability and predictability of TC activity.

1. Introduction

Tropical cyclone (TC) activity in the Atlantic basin varies considerably on the interannual time scale. A better understanding of the variability may help to improve the seasonal prediction of TC activity. Seasonal prediction, in turn, provides an effective way to test the understanding of associated physical processes. Despite the progress made in recent decades, the seasonal prediction of TC activity remains challenging. The seasonal prediction bust of Atlantic TC activity in 2013, for example, highlights our inadequate understanding of the seasonal variability of Atlantic TC activity (Vecchi and Villarini 2014; Bell et al. 2014; Zhang et al. 2016).

Tropical Atlantic climate is strongly influenced by the air–sea coupled modes in the tropics, including El Niño–Southern Oscillation (ENSO) and the Atlantic meridional mode (AMM) (e.g., Gray 1984; Kossin and Vimont 2007). The SST anomalies associated with these modes modulate Atlantic TC activity by influencing the atmospheric convection and the large-scale flow in the tropics, and the seasonal activity of Atlantic TCs often varies in concert with the tropical modes (e.g., Goldenberg and Shapiro 1996; Kossin and Vimont 2007; Vecchi and Soden 2007; Zhang and Wang 2013).

Besides the coupled tropical modes, the tropical Atlantic is also subject to the impacts of extratropical

Corresponding author e-mail: Zhuo Wang, zhuowang@illinois.edu

DOI: 10.1175/JCLI-D-16-0425.1

forcing (e.g., Czaja et al. 2002). Previous investigations of the extratropical impacts on Atlantic TC activity have mostly focused on the North Atlantic Oscillation (NAO) (Elsner 2003; Xie et al. 2005; Sabbatelli and Mann 2007; Kossin et al. 2010; Villarini et al. 2010; Colbert and Soden 2012; Kozar et al. 2012). The NAO is associated with the variability of the midlatitude jet and a meridional seesaw in sea level pressure (SLP) over the extratropical North Atlantic. It is the dominant mode of atmospheric variability over the North Atlantic in the boreal winter, but is less well defined and explains less extratropical variability in the boreal summer (Portis et al. 2001; Hurrell et al. 2003; Folland et al. 2009). Perhaps because of the NAO seasonality and different choices of the NAO indices (Pokorná and Huth 2015; Zhang et al. 2016), previous studies have not always led to consistent conclusions about how the NAO impacts Atlantic TC activity (Elsner 2003; Kossin et al. 2010; Colbert and Soden 2012). In particular, a significant simultaneous correlation between TC activity and the NAO variability remains elusive during the hurricane season (Villarini et al. 2010; Colbert and Soden 2012).

Besides the possible impacts of the NAO, extratropical frontal systems may affect Atlantic TC activity by contributing to TC formation, which is known as the tropical transition (Davis and Bosart 2003, 2004; McTaggart-Cowan et al. 2013). Notably, the tropical transition is often accompanied by potential vorticity (PV) streamers associated with anticyclonic Rossby wave breaking (RWB) (Davis and Bosart 2004; Galarneau et al. 2015). A recent study by Galarneau et al. (2015) investigated TC formation associated with the upper-tropospheric PV streamers. Based on the cases during 2004–08, they argued that the key factor determining whether a TC develops is the strength of the sea level pressure gradient and the associated lower-tropospheric moisture flux rather than the upper-level PV streamers. However, studies of RWB in the cold season have found that RWB can strongly perturb the lower troposphere and affect the SLP and the surface heat flux (e.g., Strong and Magnusdottir 2009; Michel et al. 2012), so the lower-level signals emphasized by Galarneau et al. (2015) are not necessarily independent of the upper-level streamers.

Although existing studies generally focus on how RWB facilitates TC development, there is evidence that RWB can hinder TC development. In a recent study, Zhang et al. (2016) noted that frequent RWB over the extratropical North Atlantic contributes to the tropospheric dryness and stronger vertical wind shear (VWS) over the tropical North Atlantic, which hindered the development of TCs over the tropical North Atlantic in 2013 despite its warm SST anomalies. Focusing on the month of August, Zhang et al. (2016) also found that the frequency of RWB occurrence is closely related to the variability of midlatitude jet and is negatively correlated with Atlantic TC activity (1979–2013) with high statistical significance.

In a broader context, the variability of RWB occurrence affects regional climate variability. RWB is a key ingredient associated with landfalling atmospheric rivers (e.g., Payne and Magnusdottir 2014) and affects the tropospheric moisture transport into the Arctic (e.g., Liu and Barnes 2015). The breaking of large-amplitude Rossby waves may lead to midlatitude blocking (e.g., Tyrlis and Hoskins 2008). The variability of RWB occurrence has been extensively studied in the cold season, and it has been increasingly recognized as an important process for atmospheric variability, particularly for the NAO and the hemispheric-scale annular modes (the northern and southern annular modes) (Benedict et al. 2004; Franzke et al. 2004; Rivière and Orlanski 2007; Woollings et al. 2008; Strong and Magnusdottir 2008; Wang and Magnusdottir 2011). However, RWB in the Northern Hemisphere in boreal summer has received less attention, even though RWB is more prevalent in the warm season (Postel and Hitchman 1999; Abatzoglou and Magnusdottir 2006). Meanwhile, the meridional overturning circulation in the tropics is considerably weaker in the warm hemisphere (e.g., Zhang and Wang 2013), making the circulation more prone to the impacts of extratropical eddies (e.g., Schneider and Bordoni 2008). These facts suggest that RWB in the warm season and their impacts on the tropics merit further study.

In this study, we will address the following questions. 1) What are the characteristics of RWB during the Atlantic hurricane season? 2) How does RWB modify the atmospheric conditions during the hurricane season? 3) What is the link between Atlantic TC activity and the variability of RWB occurrence, and what mechanism controls the link? To address these questions, we will use the algorithm described in Strong and Magnusdottir (2008) to study RWB during the Atlantic hurricane season for the period of 1979–2013. Compared with Zhang et al. (2016), this study extends the analyses of RWB in August to the Atlantic hurricane season and seeks to better understand the underlying mechanisms. We hope that the work can provide new insights into the interaction between the tropics and the extratropics, and advance the understanding of the variability and predictability of Atlantic TC activity.

The rest of this paper is organized as follows. Section 2 describes the data and methodology, including a brief description of the RWB detection algorithm. Section 3 characterizes RWB events during the Atlantic hurricane season and their impacts on the local environment. Section 4 explores the link between the basinwide RWB occurrence and Atlantic TC activity. The intrabasin differences (western Atlantic vs eastern Atlantic) are investigated in section 5. Section 6 addresses whether the impacts of RWB on Atlantic TCs are independent of tropical SST forcing. The last section provides a summary and discussion.

2. Data and methodology

We use global monthly and 6-hourly data on isentropic and isobaric surfaces from the European Centre for Medium-Range Weather Forecasts (ECMWF) interim reanalysis (ERA-Interim; Dee et al. 2011). The 1° monthly data are used to analyze the variations of the large-scale atmospheric environment. To reduce the computational cost of the RWB identification and exclude the small-scale PV features, the 6-hourly data of a coarser resolution (2.5°) are used to detect RWB events and to examine the associated environmental changes. In addition, the Hadley Centre Sea Ice and Sea Surface Temperature (HadISST) dataset (Rayner et al. 2003), Global Precipitation Climatology Project (GPCP) dataset (Adler et al. 2003), and Atlantic hurricane database (HURDAT2; Landsea and Franklin 2013) are also used. We focus on the July–October time frame, which accounted for a majority of hurricanes (90%) and named TCs (86%) during 1979–2013.

RWB occurs when the background flow is not adequately strong to support the propagation of linear waves. The key feature of RWB is the rapid and irreversible overturning of PV contours (McIntyre and Palmer 1983). We apply the algorithm described in Abatzoglou and Magnusdottir (2006) and Strong and Magnusdottir (2008) to search for high-PV tongues (''bay areas'') associated with the overturning of PV contours. The search is conducted on the 350-K isentropic surface, which is near the level of the upper-tropospheric jet. Once a high-PV tongue is identified, the location of its centroid and the corresponding time are saved for postprocessing. RWB often results in PV overturning at several consecutive time frames (''snapshots''), and each is counted as one occurrence in the calculation of the RWB frequency. The algorithm can identify both anticyclonic and cyclonic RWB (Thorncroft et al. 1993); we only consider anticyclonic RWB here because cyclonic RWB is infrequent equatorward of 40°N during July–October (not shown).

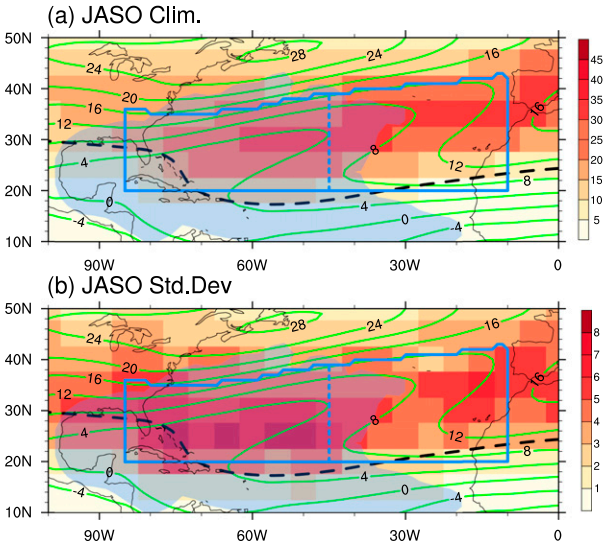

FIG. 1. (a) Seasonal mean and (b) standard deviation of the distribution of RWB-related PV tongues. The distribution was counted in 5° × 5° bins and smoothed with a 4-point averaging. The green contours show the climatology mean of the 200-hPa zonal wind ($m\,s^{-1}$). The solid blue lines highlight the domain of D0 (see section 2 for more details), which is separated into the western (Dw) and the eastern (De) subdomains by the dashed blue line (45°W). The blue shading illustrates the area that TCs frequently track through. The black dashed line outlines the 200-hPa TUTT.

To focus on the links with TC activity, our analyses are restricted to the RWB events in a domain equatorward of the midlatitude jet. The northern boundary of the domain is set at 10° latitude south of the axis of the 200-hPa climatological mean midlatitude jet, and the southern boundary is set at 20°N. The domain is outlined with the blue solid lines in Fig. 1 and referred to as D0 hereinafter. Despite some subjectivity in the domain chosen, varying the northern (southern) boundaries northward (southward) by 10° latitude does not affect our main findings.

3. Characteristics of RWB in the Atlantic hurricane season

Figure 1a shows the long-term seasonal mean (July–October) of the 200-hPa zonal wind and the frequency of RWB occurrence during 1979–2013. In agreement with previous studies (e.g., Abatzoglou and Magnusdottir 2006), anticyclonic RWB over the Atlantic is most active equatorward of the mean jet. The maximum frequency of RWB occurrence is located at about 35°N over the eastern Atlantic but more equatorward (near 30°N) over the western Atlantic, consistent with the tilt of the jet. The strongest interannual variability (Fig. 1b) occurs over the western Atlantic rather than over the eastern Atlantic. RWB also tends to occur near the climatological location of the tropical upper-tropospheric trough

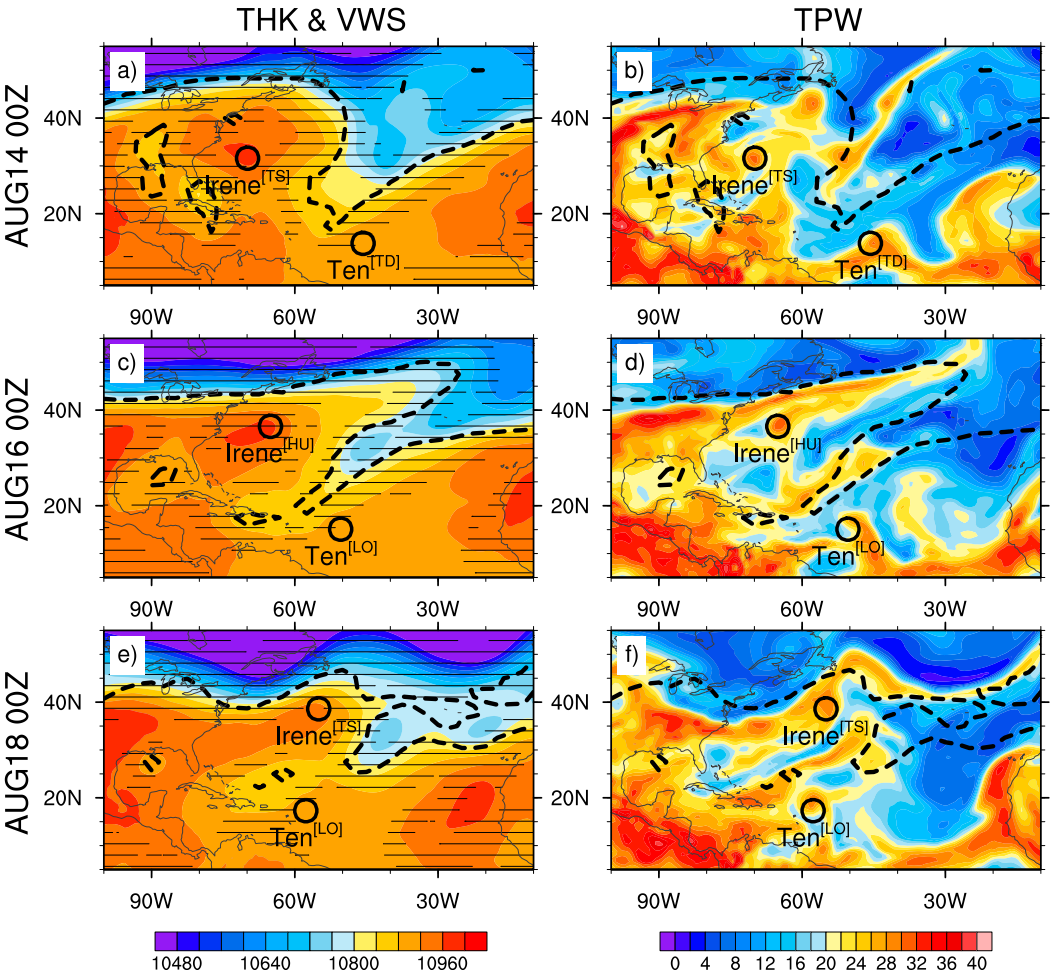

FIG. 2. A case of wave breaking in August 2005. The thick black dashed lines show the 2-PVU contour at the 350-K isentropic surface. Shown are (left) 200–850-hPa thickness (THK; m; colored shading) and VWS (values $>12\,\mathrm{m\,s^{-1}}$ shaded with pattern) and (right) total precipitable water (TPW; mm; colored shading), for 0000 UTC (a),(b) 14, (c),(d) 16, and (e),(f) 18 Aug 2005. The black circles mark tropical disturbances, with their names and categories denoted below. The storm categories (bracketed text) follow the convention of Atlantic hurricane database.

(TUTT) (Fig. 1; Postel and Hitchman 1999), which has been noted for its impacts with TC activity (e.g., Fitzpatrick et al. 1995). We next examine the characteristics of RWB and their implications for TC activity with a case study and composite analyses.

a. A case of breaking wave

Although many RWB cases have been discussed in the context of TC activity (e.g., Galarneau et al. 2015; Zhang et al. 2016), it is still helpful to start our analyses with an illustrative case in August 2005 (Fig. 2). At 0000 UTC 14 August, the 2-PVU (1 PVU = $10^{-6}\,\mathrm{K\,m^2\,s^{-1}\,kg^{-1}}$) contour on the 350-K isentropic surface (black dashed lines) suggests that a large-amplitude wave started to break over the subtropical Atlantic. In the next few days, the high-PV tongue continued to stretch southwestward and formed a cutoff low near 15°N (0000 UTC 16 August), and the cutoff low staggered in the tropics as it gradually dissipated (0000 UTC 18 August).

The breaking wave evidently affected the thickness of the 200–850-hPa layer (THK) and sharpened the gradient near the high-PV tongue (Figs. 2a,c,e), contributing to the strong VWS ($>12\,\mathrm{m\,s^{-1}}$, pattern shaded) over the subtropical and tropical Atlantic. The region also witnessed substantial changes in the moisture distribution, as indicated by total precipitable water (TPW; Figs. 2b,d,f). The TPW evolution indicates that the RWB-related mixing tends to moisten (dry) the extratropics (tropics), and the local impacts strongly depend on the position of a region relative to the breaking wave.

Figure 2 also shows that Hurricane Irene and Tropical Depression (TD) Ten were located to the

northwest and the southeast of the high-PV tongue, respectively, and that the breaking wave impacted their development rather differently. At 0000 UTC 14 August (Figs. 2a,b), Irene was located in the moist plume associated with the amplifying ridge of breaking wave, but TD Ten struggled in the dry and high-VWS environment related to the same breaking wave. After 48 h (Figs. 2c,d), Irene recurved sharply to the northeast and reached the hurricane strength at a relatively high latitude, whereas TD Ten failed to develop and evolved to a weak low. The evolutions of the two storms highlight the complex relations between RWB and TC development.

b. Composite analyses

To demonstrate the impacts of RWB on the local environment, composites of different variables were constructed with respect to the high-PV tongue centroids of RWB identified in the domain D0 (see section 2 for definition). The size of the composite domain was set to 50° × 50° (Figs. 3–5), which is sufficient to capture most breaking waves. The composite mean of 350-K PV is shown in black contours in Figs. 3–5 to highlight the breaking wave, which clearly shows a reversal of the meridional PV gradient. To illustrate the impacts of RWB on the environment, anomalies of various fields in the vicinity of PV tongues are calculated relative to their long-term seasonal mean at the corresponding locations. One-sample Student's t tests were used to determine whether the composite anomalies are significantly different from zero ($p < 0.05$).

We first examine the composite wind anomalies at 200 and 850 hPa (Figs. 3a,b). At 200 hPa, the cyclonic flow anomalies wrapping around the high-PV tongue are paired with the anticyclonic anomalies in the northwest, indicating an incoming Rossby wave. The breaking wave also shows a southwest–northeast tilt, which implies the northward transport of westerly eddy momentum. These synoptic features are expected to modulate the position and strength of the midlatitude jet (e.g., Strong and Magnusdottir 2008). The meridional component of anomalous wind, such as the strong equatorward flow anomalies along the PV tongue (>5 m s^{-1}), facilitates the tropical–extratropical mixing (e.g., Waugh and Polvani 2000). Significant wind anomalies are prevalent in the 50° composite domain, indicating that RWB impacts a broad area. In particular, the wind anomalies at 200 hPa extend 15° latitude south of the high-PV tongue centroid. Given that RWB occurs frequently in the subtropical Atlantic (Fig. 1), this southward extension suggests that some RWB events directly impact the Atlantic main development region (MDR; 10°–20°N, 20°–90°W).

At 850 hPa, the anomalous flow shows a monopole pattern in the domain, with the anticyclonic anomalies centered at about 5° latitude north of the centroid of the high-PV tongue. Despite the weak magnitude, the 850-hPa wind anomalies are statistically significant and associated with the positive anomalies in SLP (Figs. 3b, d). Figure 3d also shows negative SLP anomalies northwest of the positive anomalies. The overall SLP pattern is similar to the cold-season composites (Strong and Magnusdottir 2008), except that the anomalies are generally an order of magnitude weaker.

The anomalous wind shows some baroclinic characteristics in the northwest and the southeast of the breaking waves (Figs. 3a,b), implying that RWB may contribute to significant changes in VWS. Here we define VWS as the magnitude of the vector difference between the 200- and 850-hPa wind [$\mathrm{VWS} = \sqrt{(u_{200} - u_{850})^2 + (v_{200} - v_{850})^2}$], and positive anomalies thus represent enhanced VWS. As shown in Fig. 3c, the positive (negative) VWS anomalies generally correspond to the westerly (easterly) anomalies at 200 hPa, with the negative anomalies sandwiched by the positive anomalies. The south lobe of positive VWS anomalies, located at about 8° latitude south of the PV tongue centroid, may directly impact TCs or their precursors when RWB occurs at low latitudes. If one considers the subsequent drift of RWB residuals, the area influenced by RWB would likely be broader.

RWB is also associated with significant anomalies in the vertical motion (ω). Figure 4 shows the composites of vertical motion anomalies associated with RWB at three isobaric levels (300, 500, and 700 hPa). The patterns at these levels are largely consistent, featuring upward (downward) anomalies in regions of poleward (equatorward) motion. The upward anomalies in the northwest are particularly strong and appear associated with the extratropical precipitation anomalies (Fig. 4d). The related diabatic heating could amplify the upper-level ridge and affect the wave breaking process (e.g., Massacand et al. 2001). Some upper-level lifting signals also appear on the southeastern edge of breaking waves (Figs. 4a,b), but the forcing does not strongly influence the lower troposphere (Fig. 4c) and induces only weak positive precipitation anomalies. In comparison, the downward anomalies near the domain center extend through the troposphere. The anomalies are strongest at the 300-hPa level and weaken as the height decreases. The negative values of $\partial\omega/\partial p$ indicate that the downdrafts are divergent and contribute to the low-level anticyclonic anomalies, agreeing with the broad anticyclonic anomalies near the surface (Figs. 3b,d). This suggests that the upper-level forcing of RWB impacts the lower troposphere and contributes to the variability of the subtropical high.

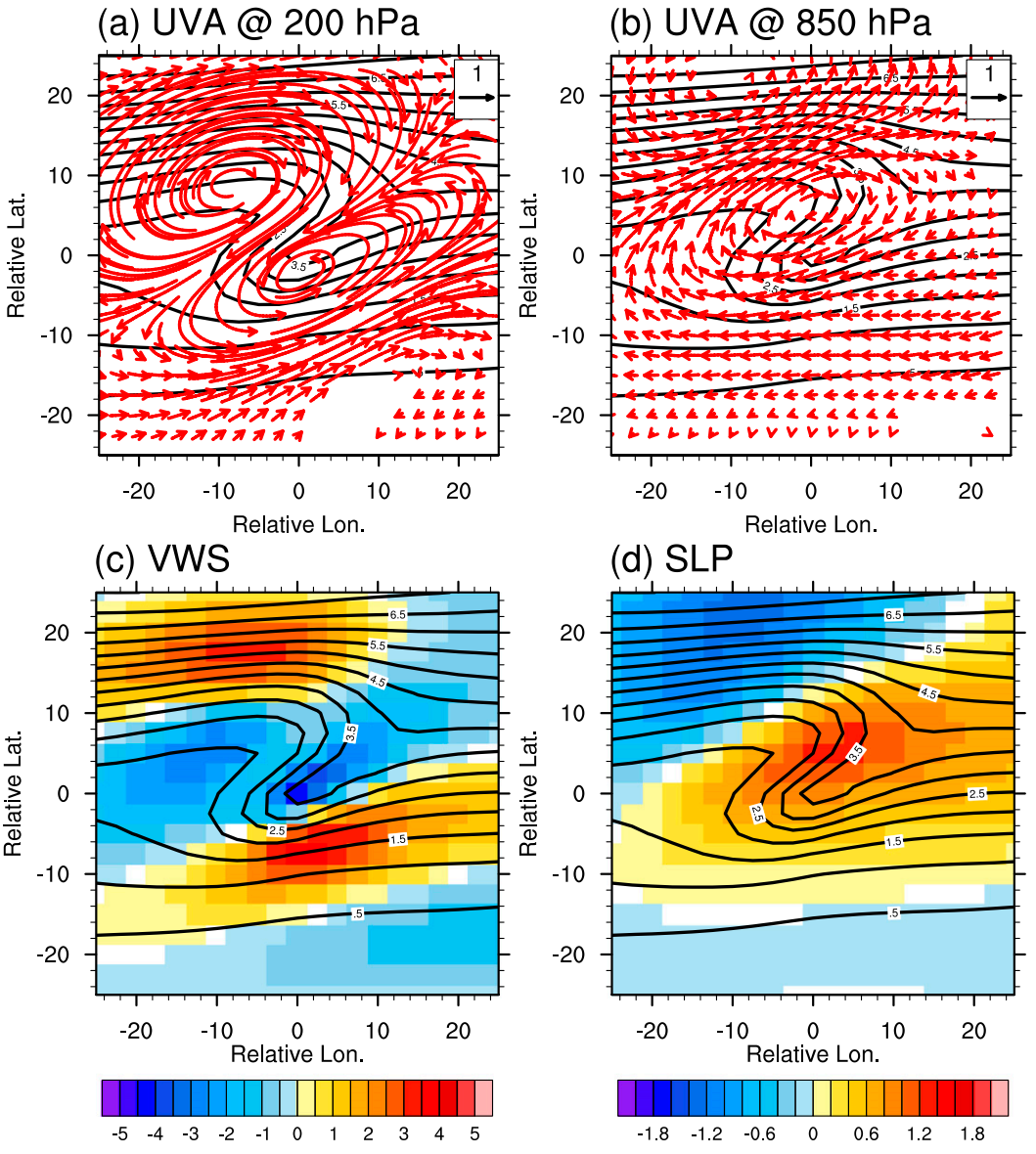

FIG. 3. Composites of anomalies in (a) 200- and (b) 850-hPa wind ($m\,s^{-1}$), (c) VWS ($m\,s^{-1}$), and (d) SLP (hPa). Black contours show the corresponding composite of PV (PVU) at the 350-K isentropic surface. In (a) and (b), the shown vectors have either a u or v component that passes the one-sample Student's t test and reaches the 95% confidence level; in (c) and (d), signals below the 95% confidence level are masked out with white.

As indicated by the precipitation anomalies, RWB also affects the moisture distribution. Figures 5a and 5b show the relative humidity (RH) anomalies at two pressure levels (500 and 850 hPa). Positive (negative) anomalies generally collocate with the anomalous upward (downward) motion (Figs. 4a–c). The RH anomalies, together with the temperature anomalies (Figs. 5c,d), affect the moisture content of the air column. The anomalies of total precipitable water (Fig. 5e) approximately follow the pattern of the low-level humidity anomalies, due to the large moisture content in the lower troposphere. Some disagreement between the 850-hPa RH and TPW, such as the signals on the southern edge of the breaking wave, can be attributed to the modulation of the saturated vapor pressure by temperature anomalies. The low-level pattern also dominates the horizontal transport of moisture (Fig. 5f). There is strong horizontal moisture flux ($>20\,kg\,m^{-2}\,s^{-1}$) associated with the low-level anticyclonic anomalous flow, especially on its northwestern side where the poleward transport prevails. The associated anomalous divergence (convergence) of the moisture flux (not shown) appears to contribute to the

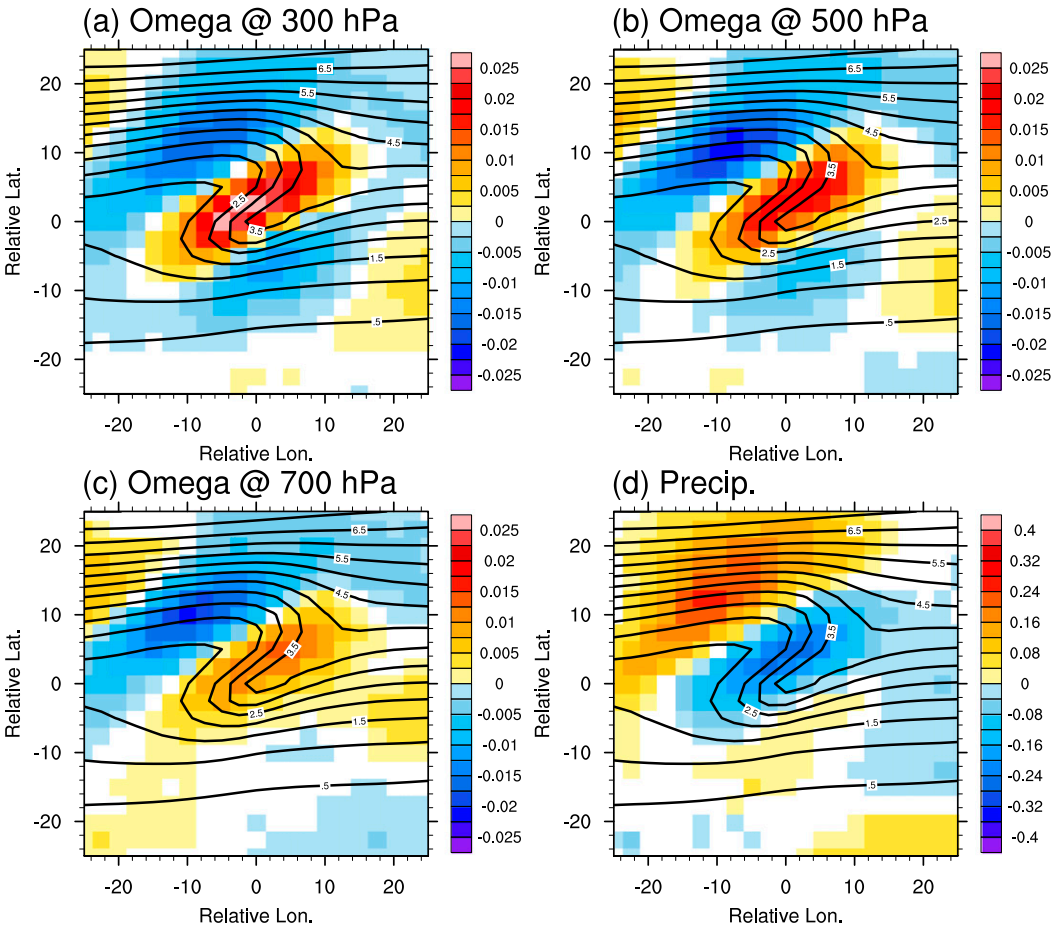

FIG. 4. Composites of anomalies in (a) 300-, (b) 500-, and (c) 700-hPa ω (Pa s^{-1}), and (d) precipitation (from ERA-Interim; mm). The black contours and white masking follow Fig. 3.

negative (positive) anomalies of total precipitable water (Fig. 5e) and precipitation (Fig. 4d).

In summary, RWB events strongly affect the North Atlantic environment during the hurricane season. These RWB events facilitate three-dimensional mixing and affect both dynamical (e.g., VWS) and thermodynamical (e.g., moisture) variables throughout the troposphere. The findings are consistent with previous studies (e.g., Strong and Magnusdottir 2009) and strongly suggest that RWB can impact convective systems, including TCs and their precursors (Fig. 2; Davis and Bosart 2003, 2004; Galarneau et al. 2015; Zhang et al. 2016). Different from Galarneau et al. (2015), we note that the dry subsidence associated with the upper-level RWB extend throughout the troposphere, directly impacting the wind anomalies and moisture transport in the lower troposphere.

4. Variability of RWB occurrence and TC activity: Basinwide perspective

How RWB affects TC development involves competing physical processes (Leroux et al. 2016) and is often obscured by transient features. Studying a large number of cases is thus very demanding and likely undermined by the subjectivity in analyses. Recognizing these obstacles, we instead take a statistics-oriented approach to explore the climatological relation between RWB occurrence and TC activity.

a. Correlation and composite analyses

To represent the basinwide RWB occurrences, we define two seasonal indices, RWBFreq and RWBArea, within the domain D0 (Fig. 1). The former index represents the total number of RWB occurrences over a season, and the latter is defined as the sum of high-PV tongue areas. The two seasonal indices are strongly correlated during 1979–2013 ($r \approx 0.87$), and our discussion will mainly focus on RWBFreq for brevity. TC activity is represented by three indices, the hurricane count (HURR; wind speed $\geq$33 m s^{-1}), the count of named TCs (TCN; wind speed $\geq$17.5 m s^{-1}), and the accumulated cyclone energy (ACE; Bell et al. 2000). The ACE is defined as the sum of the squares of

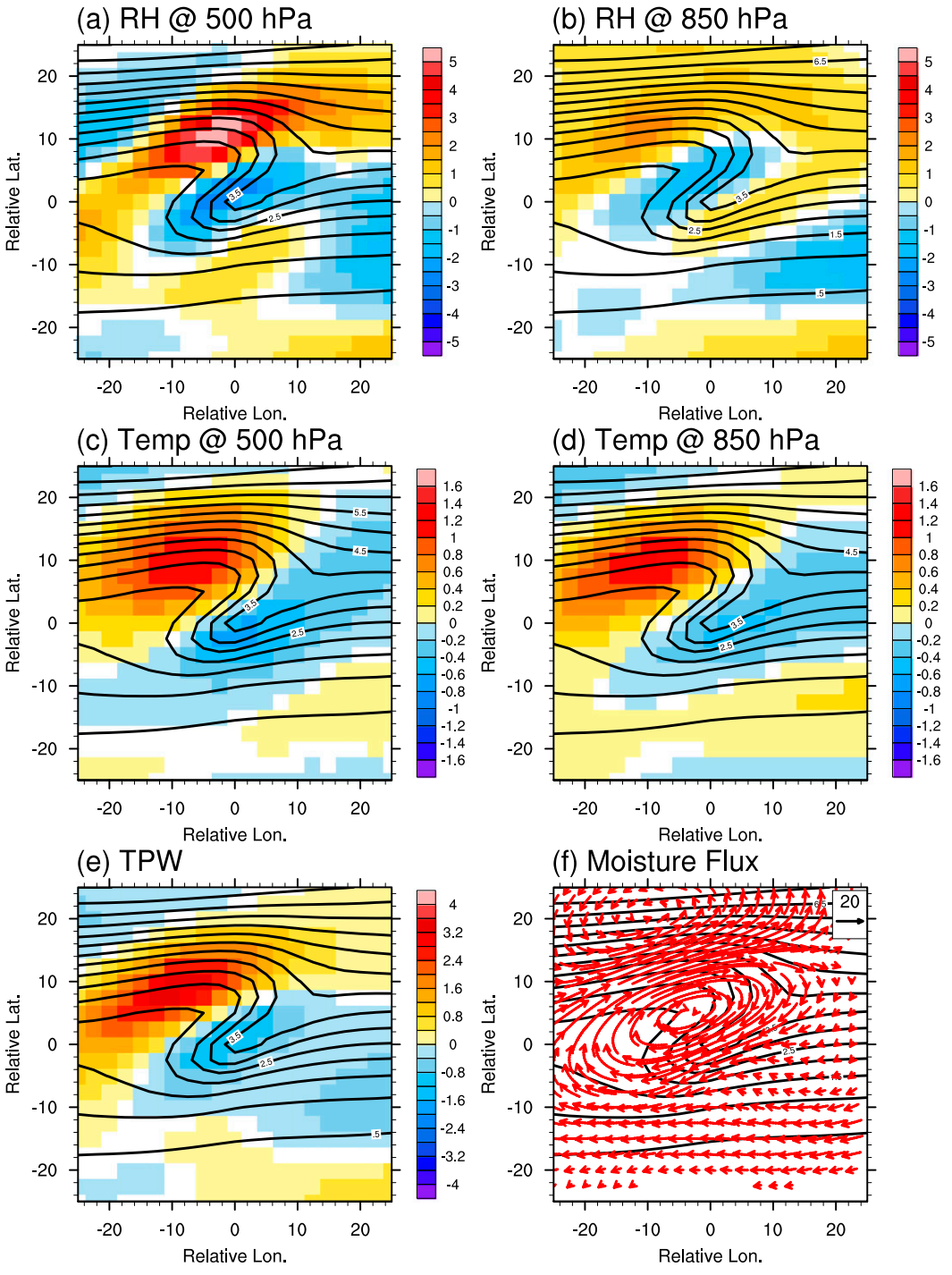

FIG. 5. Composites of anomalies in (a) 500- and (b) 850-hPa RH (%), (c) 500- and (d) 850-hPa temperature (K), (e) TPW (mm), and (f) column integrated moisture flux (kg m^{-2} s^{-1}). The black contours, red vectors, and white masking are as in Fig. 3.

maximum sustained surface wind speed estimated every 6 h for all the named TCs. All the three indices are calculated based on the storms that formed in July–October.

Table 1 shows that RWBFreq and RWBArea are negatively correlated with all the three TC indices with high statistical significance ($p < 0.01$). The correlation is particularly strong between RWBFreq and HURR

TABLE 1. Correlation between the basinwide RWB indices and Atlantic TC activity. The RWB indices are RWBFreq and RWBArea of RWB-related PV tongues identified in D0 (see Fig. 1). The TC activity indices are HURR, TCN, and ACE. The MDR SST is the SST average in 10°–20°N, 20°–90°W; the Niño-3.4 index is the SST average over 5°N–5°S, 120°–170°W. All the correlation coefficients are above the 95% confidence level.

	HURR	TCN	ACE
RWBFreq	−0.67	−0.48	−0.73
RWBArea	−0.62	−0.45	−0.65
MDR SST	0.64	0.57	0.65
Niño-3.4	−0.42	−0.34	−0.37

($r \approx -0.67$) or ACE ($r \approx -0.73$). For comparison, Table 1 includes correlations with the mean SST in the MDR and the Niño-3.4 index. Both indices represent prominent modulators of Atlantic TC activity and are commonly used predictors in statistical models for TC prediction. Notably, the correlations of the TC indices with RWBFreq are comparable to their correlations with the MDR SST and stronger than those with the Niño-3.4 index. The negative correlations in Table 1 (rows 2 and 3) suggest that frequent occurrences of RWB are associated with suppressed TC activity on the seasonal scale, even though the PV remnants of RWB can occasionally promote TC formation (e.g., Davis and Bosart 2004).

The composite analysis was carried out to further illustrate the impacts of RWB on Atlantic TC activity. Based on the RWBFreq index, we select 8 years with the most frequent occurrences of RWB and 8 years with the least frequent occurrences of RWB (see the caption of Fig. 6), and refer to the two groups as RWBFreq(+) and RWBFreq(−), respectively. Figure 6 shows a strong contrast in TC frequency, intensity, and tracks between the two groups. There are fewer TCs forming in the MDR in the RWBFreq(+) group than in the RWBFreq(−) group; TCs in the RWBFreq(+) group are generally less intense, have shorter tracks, and make fewer landfalls. More specifically, the RWBFreq(+) group has 87 TCs, 31 (35.6%) of which reach hurricane strength, and the average lifetime of the TCs is only 91 h. In contrast, the RWBFreq(−) group contains 127 storms, 70 (55.1%) of which reach hurricane strength, and the TCs on average have a lifetime of 139 h.

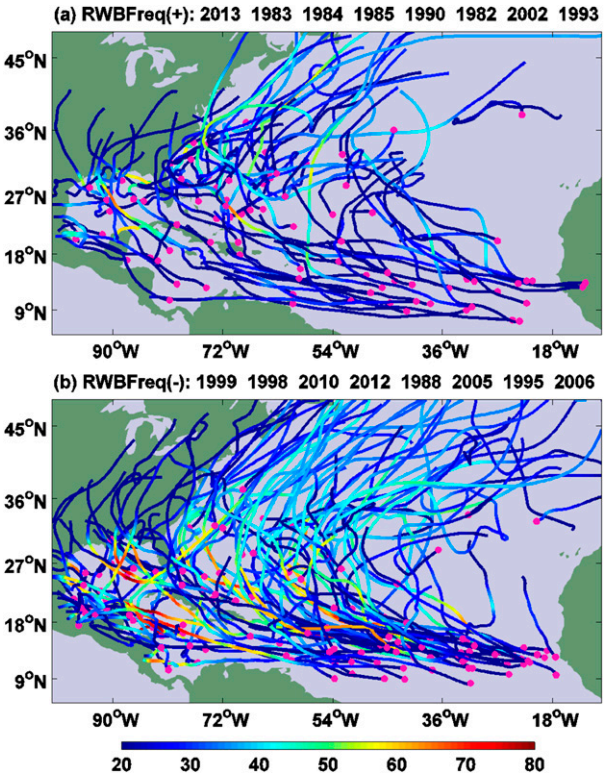

FIG. 6. Composite of TC tracks of (a) RWBFreq(+) group and (b) RWBFreq(−) group. The pink dots highlight the locations of TC genesis, and the coloring represents the wind speed (m s^{-1}) of TCs. The composite members of each group are denoted in the subplot titles.

b. Physical mechanisms

This section investigates the physical mechanisms underlying the statistical relationships between the variability of RWB occurrence and Atlantic TC activity. We have shown in section 3 that RWB modulates the local moisture and VWS distribution on the synoptic scale. To illustrate the link between the synoptic-scale variability and the variations in the seasonal mean states, a two-dimensional probability distribution function (PDF) was constructed for precipitable water (PW) and VWS using the 6-hourly data. We focus on the tropical North Atlantic region (10°–25°N, 10°–85°W), which TCs frequently track through and which is often to the south of breaking waves (Fig. 1).

Figures 7a and 7b show the two-dimensional PDF composites of RWBFreq(+) and RWBFreq(−), respectively. The distributions of PW and VWS in both groups have a wide range, which is consistent with the rich spatial and temporal variability in the region (e.g., easterly waves and dry air outbreaks). The composite difference (Fig. 7c) shows that the concurrent occurrence of dry air and high VWS, corresponding to the upper-left corner in the PW–VWS space, increases when RWB occurs more frequently. The relation between tropospheric moisture and VWS, as well as its link with RWB, is consistent with the conditions found in the south of breaking waves (Figs. 3 and 5). It also agrees

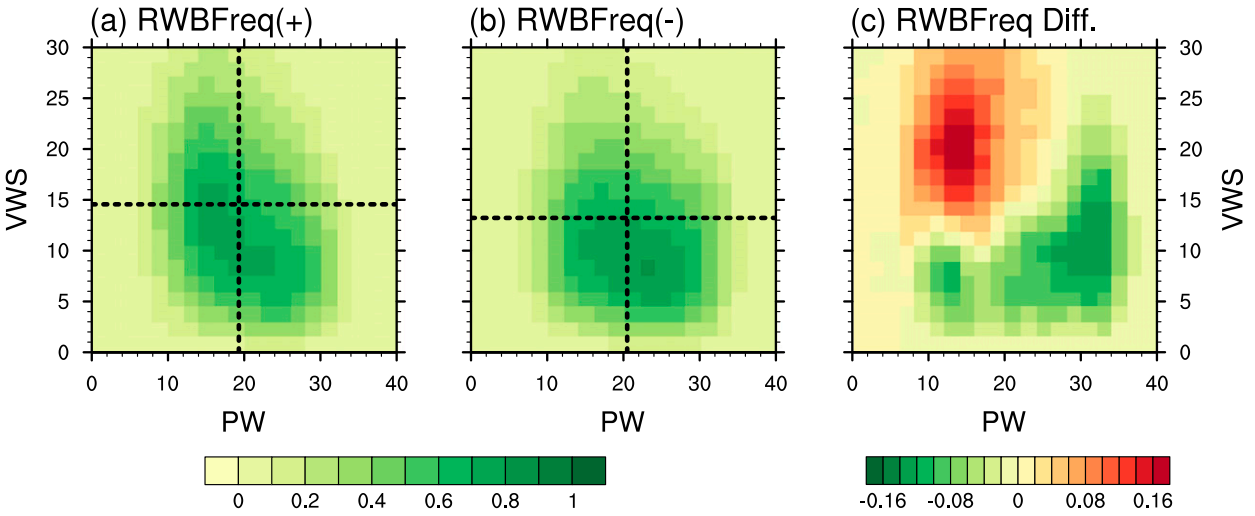

FIG. 7. Two-dimensional PDFs (%) of PW and VWS for the (a) RWBFreq(+) and (b) RWBFreq(−) groups, and (c) their differences [RWBFreq(+) minus RWBFreq(−)]. PW (mm) and VWS ($m\,s^{-1}$) are calculated for the tropical North Atlantic (10°–25°N, 10°–85°W). In (a) and (b), the horizontal (vertical) dashed black lines denote the mean value of VWS (PW) in the corresponding groups.

with the analyses of tropical Atlantic atmosphere in Dunion (2011), which shows that air of extratropical origin, when compared to tropical-origin air, is drier and accompanied by higher VWS during the hurricane season.

Figures 7a and 7b also show considerable differences in seasonal mean VWS (~1.6 $m\,s^{-1}$) and PW (~1 mm) (black dashed lines), indicating that the RWB-related synoptic variability has ties to the seasonal mean variability. To further demonstrate the link, we examined the spatial variations of seasonal mean PW, precipitation, VWS, and SST in Fig. 8. All four selected variables show significant composite differences in the tropical North Atlantic. When RWB occurs more frequently, PW and precipitation decrease over the tropical North Atlantic and the West Africa; meanwhile, VWS increases and SST decreases in the tropical North Atlantic region. These variations are consistent with suppressed TC activity (Fig. 6) in the Atlantic basin (e.g., Gray 1990; DeMaria 1996; Klotzbach and Gray 2009). It is also worth noting the variations in VWS (2–7 $m\,s^{-1}$), when compared to the climatological mean (green contours), appear much more pronounced than variations in PW (0.4–2.0 mm).

In summary, our analysis illustrates that the environmental variations associated with RWB strongly modulate Atlantic TC activity. When RWB occurs more (less) frequently, the tropical North Atlantic is subject to stronger (weaker) VWS, as well as reduced (increased) PW, precipitation, and SST. These variations, although not necessarily all directly driven by RWB (see section 6), contribute to a strong and negative correlation between the frequency of RWB occurrence and Atlantic TC activity.

5. Variability of RWB occurrence and TC activity: Intrabasin contrast

We will examine RWB over the western and the eastern Atlantic separately in this section. RWB occurs upstream of the midlatitude jet core over the western Atlantic and downstream over the eastern Atlantic (Fig. 1). The incoming Rossby waves in the two subdomains may have different sources and paths, and their breaking may be associated with different aspects of jet variability (e.g., Drouard et al. 2013, 2015). Furthermore, the locations of breaking waves relative to the TC distribution are different in the two subdomains, which could affect how breaking waves influence the TC development (e.g., Fig. 2). Consequently, the variability of RWB occurrence over the western and that over the eastern Atlantic are not necessarily closely related, and their impacts on TC activity may also differ. This warrants separate investigations of the two subdomains.

a. *Correlation and composite analyses*

We divide the North Atlantic domain (D0) into a western (Dw) and an eastern (De) subdomain along the 45°W longitude line (Fig. 1). Although the choice of the dividing line is subjective, changing its longitude by ±10° does not alter our main results. We denote the frequency of RWB occurrence in the western and the eastern subdomains as RWBw and RWBe, respectively. The insignificant correlation between RWBw and RWBe ($r \approx 0.27$; Table 2) suggests that the variability of RWB occurrence in the two subdomains is rather independent. Table 2 also shows the correlations between

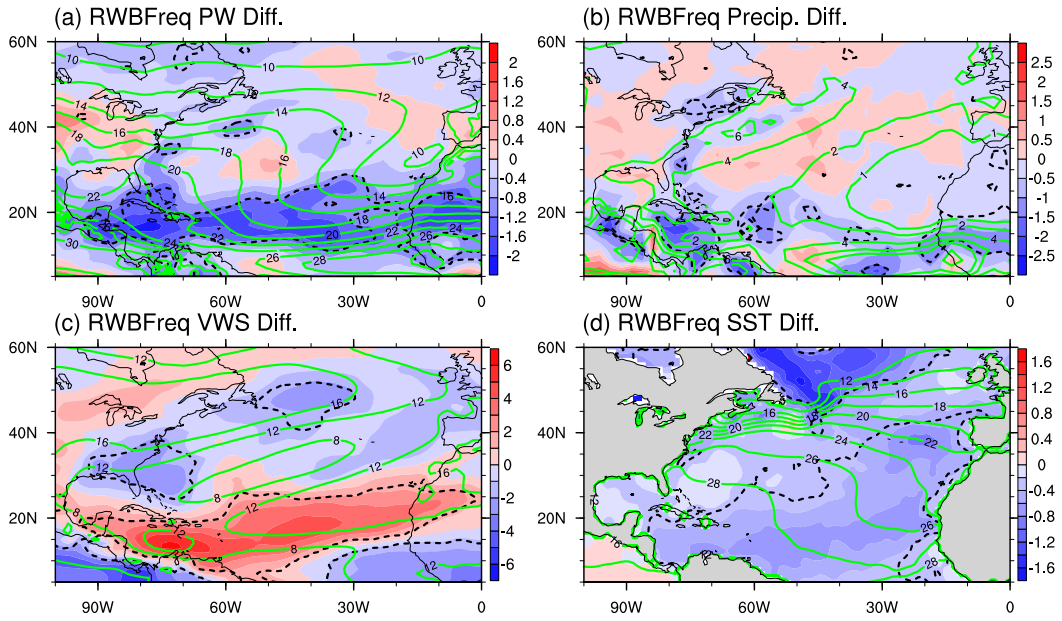

FIG. 8. Composite differences [RWBFreq(+) minus RWBFreq(−)] of the seasonal mean (a) PW (mm), (b) precipitation (from GPCP; mm day^{-1}), (c) VWS (m s^{-1}), and (d) SST (°C) that are derived from monthly data. The green contours show the 1981–2010 climatology; black dashed lines highlight the parts above the 95% confidence level.

the subdomain indices and the basinwide frequency index of RWB (RWBFreq). The stronger correlation between RWBw and RWBFreq ($r \approx 0.90$), along with the larger standard deviations of RWB occurrence in Dw (Fig. 1b), suggests that the western basin makes a larger contribution to the basinwide variability. The results prompted us to calculate and compare the correlations of RWBw and RWBe with TC activity (Table 2). Similar to RWBFreq, RWBw is highly correlated with the basinwide hurricane count, TC count, and ACE. In contrast, RWBe has much weaker correlations with the three TC indices, and only the correlation with the ACE is statistically significant ($p < 0.05$). This supports the notion that RWB over the western Atlantic has a different impact on TC activity than RWB over the eastern Atlantic.

The contrast between RWBw and RWBe can be further illustrated by the composite analysis of TC tracks (Fig. 9). The composites are constructed similarly to those in Fig. 5, except that the track density function (Xie et al. 2005) is shown to facilitate comparison and significance testing. The RWBw-associated variability of TC tracks closely resembles the variability associated with RWBFreq (not shown). When RWB occurs frequently over the western Atlantic (Dw), the track density is reduced over most of the basin. The most statistically significant signals are found south of 25°N, with some scattered in the midlatitude (Fig. 9e). In contrast, the RWBe-associated variability is generally weaker and much less coherent in the tropics (Fig. 9f). Some statistically significant differences of TC tracks are found over the extratropical western Atlantic, suggesting a shift of storm tracks and less landfalling TCs on the east coast of the United States when RWB occurs frequently in the eastern basin.

b. *Physical interpretations*

We now investigate why RWBw is more strongly correlated with TC activity. One possibility is that RWB events in the two subdomains (Dw and De) have different characteristics (e.g., Galarneau et al. 2015) and thus impact TC activity differently. We examined the composites of RWB events in the two subdomains separately (figures not shown). In general, RWB in both subdomains shows patterns similar to those in Figs. 3 and 4, although some statistically significant differences

TABLE 2. Correlation between the variability of RWB occurrence in two subdomains and Atlantic TC activity. RWBw and RWBe are the total frequency of RWB-related PV tongues identified in Dw and De (see Fig. 1), respectively. The indices of TC activity are the same as in Table 1. The correlation coefficients above the 95% confidence level are indicated with asterisks.

	RWBw	RWBFreq	HURR	TCN	ACE
RWBw	—	0.90*	−0.66*	−0.56*	−0.68*
RWBe	0.27	0.67*	−0.33	−0.10	−0.43*

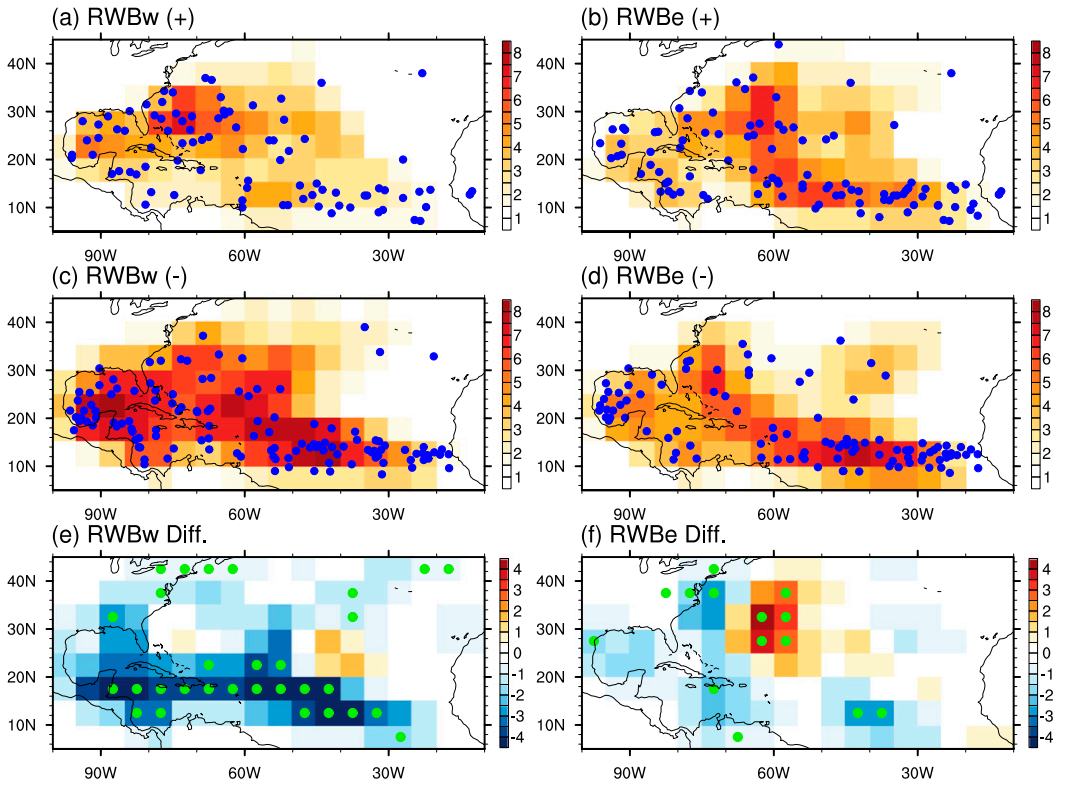

FIG. 9. Composites of TC track density: (a) RWBw(+) group, (c) RWBw(−) group, and (e) their difference; and (b) RWBe(+) group, (d) RWBe(−) group, and (f) their difference. The blue dots in (a)–(d) highlight the genesis locations. The green dots in (e) and (f) highlight the track density difference above the 90% confidence level.

between the two subgroups are present. For example, the western basin events are accompanied by a weaker high-PV tongue and weaker VWS anomalies in their southeast, but are associated with stronger precipitation anomalies and surface anticyclonic anomalies. These differences are qualitatively consistent with the description in Galarneau et al. (2015). Based on the intrabasin differences, Galarneau et al. (2015) suggested that the western basin RWB is more favorable for tropical transition. This thus does not explain the stronger negative correlations between RWBw and the Atlantic TC indices (Table 2).

Another possibility for the stronger impacts of RWBw on TC activity is related to the different spatial distributions of RWB events with respect to TC tracks over the western and eastern Atlantic. As shown in Fig. 1, the regions frequented by both RWB and TCs are mostly found in the western basin, and the large variability of RWB is closer to TC tracks over the western Atlantic than over the eastern Atlantic. RWB over the western Atlantic can thus more effectively hinder the development of a TC precursor or the intensification of an existing TC. In contrast, RWB over the eastern Atlantic generally occurs more poleward of TC tracks. The spatial proximity of RWB to TC distributions indicates that RWB in the western basin more readily influences TCs. In addition, even though RWB in the eastern basin may hinder the development of a tropical disturbance, the disturbance still has a chance to develop downstream if the environmental conditions are favorable in the western basin. The breaking wave in Fig. 2, for example, hindered the development of TD Ten over the central Atlantic, but the remnant of TD Ten later merged with a tropical wave and developed into Hurricane Katrina over the Caribbean Sea (Knabb et al. 2005). This explains why RWBe is weakly correlated with the TC number but has a stronger (although still moderate) correlation with the hurricane counts or the ACE (Table 2).

The seasonal mean variations of VWS and moisture also prove useful in explaining the contrast related to RWBw and RWBe. Figure 10 showed that the VWS and PW variations associated with RWBw are similar to those associated with RWBFreq, while the coherent and significant signals associated with RWBe mostly appear near western Europe and North Africa and are rather limited over the tropical Atlantic. The stronger link between RWBw and the environmental variability of the tropical Atlantic thus also helps to

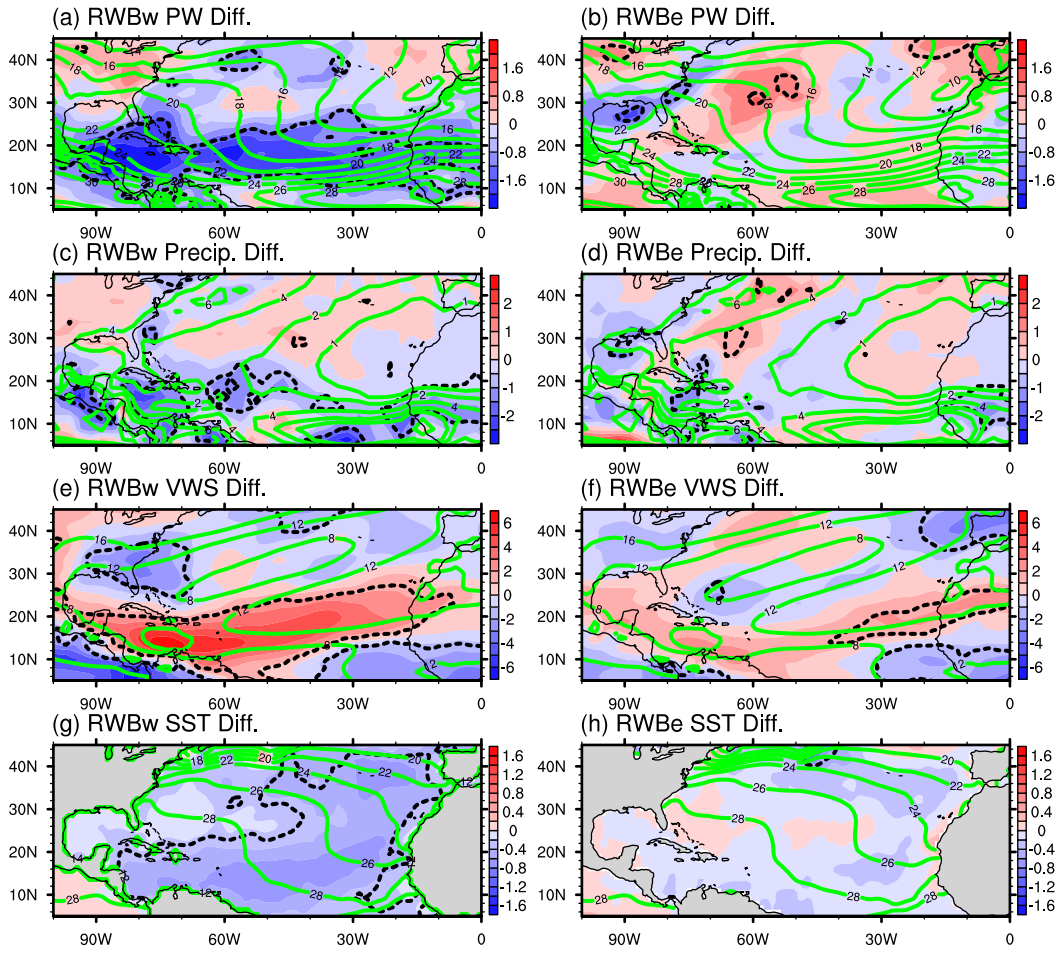

FIG. 10. As in Fig. 8, but for (left) RWBw and (right) RWBe.

explain the stronger correlation between RWBw and TC activity.

6. Impacts of tropical and extratropical variability on TC activity

RWB is related to both extratropical and tropical variability of the climate system. For example, the variability of RWB occurrence in the cold season has been linked to the phase transition and maintenance of the NAO (e.g., Rivière and Orlanski 2007; Woollings et al. 2008; Strong and Magnusdottir 2008). Meanwhile, the basic state on which Rossby waves propagate can be influenced by the tropical SST (e.g., Orlanski 2005; Drouard et al. 2015). Consistently, RWBFreq is highly correlated with the leading extratropical modes (see later discussion), the MDR SST ($r = -0.61$), and the Niño-3.4 index ($r = 0.36$). This leads to the question whether the impacts of RWB, as documented in previous sections, simply reflect the indirect impacts of tropical forcing.

To address the above question, we calculated the partial correlations (Stuart et al. 2009) between selected "forcing" indices X_i and large-scale environmental variables Y_j. The forcing indices X_i considered here are the MDR SST, the Niño-3.4, and RWBFreq, and the environmental variables Y_j are PW, VWS, and THK of the 200–850-hPa layer. Assuming one is interested in the relation between a forcing index X_1 and an environmental variable Y_1, the calculation of their partial correlation follows a two-step procedure: 1) removing the effects of the other forcing indices (X_2 and X_3) from X_1 and Y_1 using multivariate linear regression, and 2) evaluating the Pearson correlation coefficient of the residuals of index X_1 and variable Y_1. This provides insight into how one forcing index X_1 independently affects the environmental variable Y_i, while the effects of other forcing indices are controlled. The partial correlation relations are shown in Fig. 11.

Figures 11a–c suggest that the local SST is the major contributor to the seasonal variability of PW over the

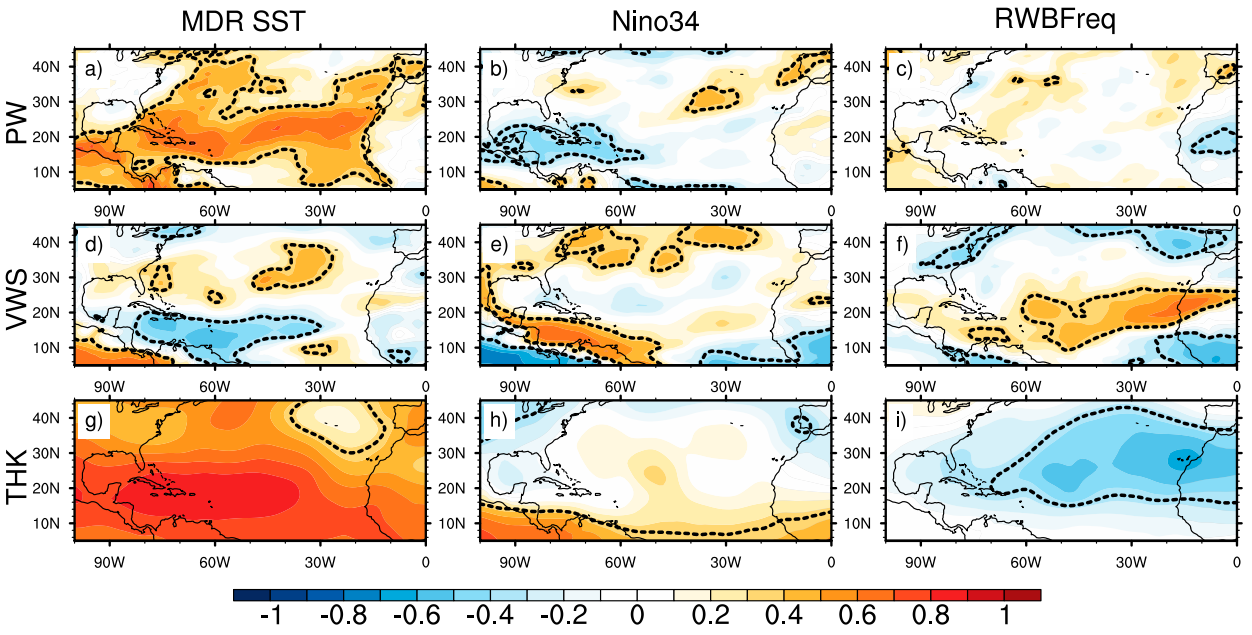

FIG. 11. Partial correlation between climate "forcing" indices and seasonal means of different environmental variables. The indices include (left) MDR SST, (center) Niño-3.4, and (right) RWBFreq. The seasonal means are (top) PW, (middle) VWS, and (bottom) THK. Black dashed lines highlight the parts above the 95% confidence level.

tropical North Atlantic. Consistent with the strong local impacts of tropical SST on tropospheric moisture (e.g., Wentz and Schabel 2000), the correlation maps show that warm SST anomalies in the MDR correspond to higher moisture content over the tropical and subtropical North Atlantic. The impacts of the ENSO on PW are mainly restricted near the Greater Antilles, with lower PW values over the tropical North Atlantic associated with warm anomalies of the Niño-3.4 SST. The link between the ENSO and the Caribbean climate, as noted by many studies, is also manifested in precipitation variations (e.g., Giannini et al. 2000). In contrast, RWBFreq does not seem to independently modulate the seasonal mean PW over the tropical North Atlantic (Fig. 11c). Based on these findings, the mean tropical PW variations in Fig. 8a appear mainly contributed by the local SST variations (Fig. 8d).

Figures 11d–f suggest that all the three so-called forcing indices can independently modulate VWS in the tropics. The partial correlations show that warm anomalies of the MDR SST tend to reduce VWS in the MDR but enhance VWS between 20° and 40°N. ENSO mainly modulates VWS over the Caribbean Sea, and its impact on the rest of the MDR is very limited. These SST–VWS relationships are consistent with the extensive preceding studies (e.g., Goldenberg and Shapiro 1996; Sutton and Hodson 2007; Zhang and Wang 2013). Meanwhile, we note that RWBFreq is positively correlated with VWS over a majority of the MDR, with statistically significant signals located over the Caribbean Sea and the eastern and central MDR (Fig. 11f). The partial correlation pattern notably resembles the RWBFreq-associated VWS variations (Fig. 8c), indicating that the VWS variations reflect considerable extratropical influences.

Through the thermal wind relation, the seasonal mean VWS variations can be related to THK changes (e.g., Allen and Sherwood 2008). The MDR SST, for example, is strongly correlated with THK near 20°N over the western Atlantic. The positive correlation probably arises from the SST-related precipitation variations, which influence the air column thickness through diabatic heating. The THK changes associated with the ENSO have a very different spatial pattern, with statistically significant signals largely confined to the deep tropics (equatorward of 15°N). In contrast, the THK signals associated with RWBFreq mainly appear between 20° and 40°N, showing a negative correlation between THK and RWBFreq. The facts are consistent with the strong equatorward mixing of cold extratropical air facilitated by frequent RWB (e.g., Zhang et al. 2016). The associated thickness variations affect the THK gradient in the MDR and contribute to the variability of VWS (Fig. 11f), supporting the idea that VWS in the tropics is subject to extratropical impacts.

The variability of RWB occurrence in the winter season has been linked to the variability of extratropical storm track (e.g., Rivière and Orlanski 2007). It is

reasonable to expect that the variability of RWB occurrence in the hurricane season is also associated with extratropical dynamics. We indeed found that RWBFreq is significantly correlated with the extratropical modes, such as the North Atlantic Oscillation ($r = 0.42$) and the east Atlantic pattern ($r = -0.43$) (Barnston and Livezey 1987). These relations and the implications for the extratropical climate will be addressed in an upcoming study.

Overall our analyses suggest that the variability of RWB occurrences can strongly modulate some key aspects of the tropical environment (e.g., temperature and VWS) independent of tropical SST forcing in the Atlantic MDR and the Niño-3.4 region. On the other hand, the tropical SST dominantly influences the variations of PW on the seasonal scale (Fig. 8a), although RWB strongly regulates the moisture distribution on the synoptic scale (section 3). These facts indicate that extratropical forcing, in addition to tropical forcing, is involved in the variability of Atlantic TC activity (Fig. 6 and Table 1).

7. Summary and discussion

Much effort has been dedicated to understanding the variability and predictability of Atlantic TC activity in the past decades. Compared with the extensively studied tropical forcing, the extratropical impacts on TC activity have received less attention. This study investigated the impacts of extratropical RWB on tropical regions during the Atlantic hurricane season. The findings indicate that the extratropical processes associated with RWB are an important contributor to the variability of Atlantic TC activity.

This study focuses on the anticyclonic RWB identified during July–October, the peak of hurricane season. A case study and composite analyses show that RWB affects the dynamic and thermodynamic variables of the atmosphere on the synoptic scale, which include but are not limited to SLP, VWS, and moisture. Despite being generally weaker than their cold-season counterparts, the perturbations caused by breaking waves could extend throughout the troposphere.

Although previous studies suggest that the PV streamers associated with anticyclonic RWB may occasionally lead to TC formation (e.g., Davis and Bosart 2004; Galarneau et al. 2015), our findings show that the overall impact of anticyclonic RWB on seasonal TC activity is negative. Composite analyses show that fewer TCs develop when RWB occurs frequently and that these TCs are generally less intense, have a shorter lifetime, and are less likely to make landfalls. The correlations of TC activity (hurricane counts, TC counts, and the ACE) with the RWB occurrence (RWBFreq and RWBArea) during 1979–2013 are negative with high statistical significance ($p < 0.01$). The correlations are comparable to the corresponding correlations with the MDR SST index, and stronger than those with the Niño-3.4 index. The strong correlations between RWB on Atlantic TC activity can be explained by the variability of the large-scale circulation and the thermodynamic variables associated with RWB.

In addition, breaking waves over the western (Dw) and the eastern Atlantic (De) were separately examined. The variability of RWB occurrence in the western and the eastern subdomains is weakly correlated with each other, indicating different forcing mechanisms. The variability of RWB occurrence over the western Atlantic is closely correlated with Atlantic TC activity. Its eastern basin counterpart, in contrast, has a moderate correlation with the ACE but does not significantly affect the basinwide TC counts. Although breaking waves in the two subdomains are somewhat different, the intrabasin contrast can be largely attributed to the fact that western basin RWB generally occurs closer to the central portion of TC tracks and is more likely to affect TC intensification or reduce its lifetime.

We do recognize that both tropical variability and extratropical variability can influence RWB. To examine whether the impacts of RWB on Atlantic TC activity can be independent of tropical SST forcing, a partial correlation analysis was carried out to evaluate how environmental variables change with different ''forcing'' indices (section 6). It was shown that RWB can modulate tropical Atlantic environment (e.g., VWS and temperature) independent of the SST forcing in the Atlantic MDR and the Niño-3.4 region. The analyses also suggest that the extratropical impacts on the tropical large-scale environment may be comparable to the variations forced by tropical climate modes in certain aspects.

The findings here extend the existing studies of RWB and underscore the role of RWB in tropical–extratropical interaction and regional climate variability in the warm season. Since RWB is sensitive to both the variations of the upstream disturbances and the mean flow on which Rossby waves propagate (e.g., Orlanski 2005), the variability of RWB occurrence may be sensitive to different forcing sources and related to both tropical and extratropical processes. A better understanding of the forcing mechanism(s) of RWB occurrence, which is the topic of an ongoing study, will help to better understand the variability and predictability of Atlantic TC activity and other aspects of regional climate.

Acknowledgments. The study is supported by NOAA Grants NA15NWS4680007 and NA16OAR4310080,

and NRL Grant N00173-15-1-G004. We thank the NCAR Computational and Information Systems Laboratory (CISL) for providing computing resources and the ECMWF for making the ERA-Interim data publically available. We are grateful to the editor and three anonymous reviewers for their constructive comments and suggestions that helped to improve the manuscript.

REFERENCES

Abatzoglou, J. T., and G. Magnusdottir, 2006: Planetary wave breaking and nonlinear reflection: Seasonal cycle and interannual variability. *J. Climate*, **19**, 6139–6152, doi:10.1175/JCLI3968.1.

Adler, R. F., and Coauthors, 2003: The version-2 Global Precipitation Climatology Project (GPCP) monthly precipitation analysis (1979–present). *J. Hydrometeor.*, **4**, 1147–1167, doi:10.1175/1525-7541(2003)004<1147:TVGPCP>2.0.CO;2.

Allen, R. J., and S. C. Sherwood, 2008: Warming maximum in the tropical upper troposphere deduced from thermal wind observations. *Nat. Geosci.*, **1**, 399–403, doi:10.1038/ngeo208.

Barnston, A. G., and R. E. Livezey, 1987: Classification, seasonality and persistence of low-frequency atmospheric circulation patterns. *Mon. Wea. Rev.*, **115**, 1083–1126, doi:10.1175/1520-0493(1987)115<1083:CSAPOL>2.0.CO;2.

Bell, G. D., and Coauthors, 2000: Climate assessment for 1999. *Bull. Amer. Meteor. Soc.*, **81**, S1–S50, doi:10.1175/1520-0477(2000)81[s1:CAF]2.0.CO;2.

——, C. W. Landsea, S. B. Goldenberg, R. J. Pasch, E. S. Blake, J. Schemm, and T. B. Kimberlain, 2014: The 2013 North Atlantic hurricane season: A climate perspective [in "State of the Climate in 2013"]. *Bull. Amer. Meteor. Soc.*, **95** (7), S86–S90, doi:10.1175/2014BAMSStateoftheClimate.1.

Benedict, J. J., S. Lee, and S. B. Feldstein, 2004: Synoptic view of the North Atlantic Oscillation. *J. Atmos. Sci.*, **61**, 121–144, doi:10.1175/1520-0469(2004)061<0121:SVOTNA>2.0.CO;2.

Colbert, A. J., and B. J. Soden, 2012: Climatological variations in North Atlantic tropical cyclone tracks. *J. Climate*, **25**, 657–673, doi:10.1175/JCLI-D-11-00034.1.

Czaja, A., P. van der Vaart, and J. Marshall, 2002: A diagnostic study of the role of remote forcing in tropical Atlantic variability. *J. Climate*, **15**, 3280–3290, doi:10.1175/1520-0442(2002)015<3280:ADSOTR>2.0.CO;2.

Davis, C. A., and L. F. Bosart, 2003: Baroclinically induced tropical cyclogenesis. *Mon. Wea. Rev.*, **131**, 2730–2747, doi:10.1175/1520-0493(2003)131<2730:BITC>2.0.CO;2.

——, and ——, 2004: The TT problem: Forecasting the tropical transition of cyclones. *Bull. Amer. Meteor. Soc.*, **85**, 1657–1662, doi:10.1175/BAMS-85-11-1657.

Dee, D. P., and Coauthors, 2011: The ERA-Interim reanalysis: Configuration and performance of the data assimilation system. *Quart. J. Roy. Meteor. Soc.*, **137**, 553–597, doi:10.1002/qj.828.

DeMaria, M., 1996: The effect of vertical shear on tropical cyclone intensity change. *J. Atmos. Sci.*, **53**, 2076–2088, doi:10.1175/1520-0469(1996)053<2076:TEOVSO>2.0.CO;2.

Drouard, M., G. Rivière, and P. Arbogast, 2013: The North Atlantic Oscillation response to large-scale atmospheric anomalies in the northeastern Pacific. *J. Atmos. Sci.*, **70**, 2854–2874, doi:10.1175/JAS-D-12-0351.1.

——, ——, and ——, 2015: The link between the North Pacific climate variability and the North Atlantic oscillation via downstream propagation of synoptic waves. *J. Climate*, **28**, 3957–3976, doi:10.1175/JCLI-D-14-00552.1.

Dunion, J. P., 2011: Rewriting the climatology of the tropical North Atlantic and Caribbean Sea atmosphere. *J. Climate*, **24**, 893–908, doi:10.1175/2010JCLI3496.1.

Elsner, J. B., 2003: Tracking hurricanes. *Bull. Amer. Meteor. Soc.*, **84**, 353–356, doi:10.1175/BAMS-84-3-353.

Fitzpatrick, P. J., J. A. Knaff, C. W. Landsea, and S. V. Finley, 1995: Documentation of a systematic bias in the aviation model's forecast of the Atlantic tropical upper-tropospheric trough: Implications for tropical cyclone forecasting. *Wea. Forecasting*, **10**, 433–446, doi:10.1175/1520-0434(1995)010<0433:DOASBI>2.0.CO;2.

Folland, C. K., J. Knight, H. W. Linderholm, D. Fereday, S. Ineson, and J. W. Hurrell, 2009: The summer North Atlantic Oscillation: Past, present, and future. *J. Climate*, **22**, 1082–1103, doi:10.1175/2008JCLI2459.1.

Franzke, C., S. Lee, and S. B. Feldstein, 2004: Is the North Atlantic Oscillation a breaking wave? *J. Atmos. Sci.*, **61**, 145–160, doi:10.1175/1520-0469(2004)061<0145:ITNAOA>2.0.CO;2.

Galarneau, T. J., R. McTaggart-Cowan, L. F. Bosart, and C. A. Davis, 2015: Development of North Atlantic tropical disturbances near upper-level potential vorticity streamers. *J. Atmos. Sci.*, **72**, 572–597, doi:10.1175/JAS-D-14-0106.1.

Giannini, A., Y. Kushnir, and M. A. Cane, 2000: Interannual variability of Caribbean rainfall, ENSO, and the Atlantic Ocean. *J. Climate*, **13**, 297–311, doi:10.1175/1520-0442(2000)013<0297:IVOCRE>2.0.CO;2.

Goldenberg, S. B., and L. J. Shapiro, 1996: Physical mechanisms for the association of El Niño and West African rainfall with Atlantic major hurricane activity. *J. Climate*, **9**, 1169–1187, doi:10.1175/1520-0442(1996)009<1169:PMFTAO>2.0.CO;2.

Gray, W. M., 1984: Atlantic seasonal hurricane frequency. Part I: El Niño and 30 mb quasi-biennial oscillation influences. *Mon. Wea. Rev.*, **112**, 1649–1668, doi:10.1175/1520-0493(1984)112<1649:ASHFPI>2.0.CO;2.

——, 1990: Strong association between West African rainfall and U.S. landfall of intense hurricanes. *Science*, **249**, 1251–1256, doi:10.1126/science.249.4974.1251.

Hurrell, J. W., Y. Kushnir, G. Ottersen, and M. Visbeck, 2003: An overview of the North Atlantic Oscillation. *The North Atlantic Oscillation: Climatic Significance and Environmental Impact, Geophys. Monogr.*, Vol. 134, Amer. Geophys. Union, 1–35, doi:10.1029/134GM01.

Klotzbach, P. J., and W. M. Gray, 2009: Twenty-five years of Atlantic basin seasonal hurricane forecasts. *Geophys. Res. Lett.*, **36**, L09711, doi:10.1029/2009GL037580.

Knabb, R. D., J. R. Rhome, and D. P. Brown, 2005: Tropical cyclone report for Hurricane Katrina. National Hurricane Center Rep. AL122005, 43 pp.

Kossin, J. P., and D. J. Vimont, 2007: A more general framework for understanding Atlantic hurricane variability and trends. *Bull. Amer. Meteor. Soc.*, **88**, 1767–1781, doi:10.1175/BAMS-88-11-1767.

——, S. J. Camargo, and M. Sitkowski, 2010: Climate modulation of North Atlantic hurricane tracks. *J. Climate*, **23**, 3057–3076, doi:10.1175/2010JCLI3497.1.

Kozar, M. E., M. E. Mann, S. J. Camargo, J. P. Kossin, and J. L. Evans, 2012: Stratified statistical models of North Atlantic basin-wide and regional tropical cyclone counts. *J. Geophys. Res.*, **117**, D18103, doi:10.1029/2011JD017170.

Landsea, C. W., and J. L. Franklin, 2013: Atlantic hurricane database uncertainty and presentation of a new database format. *Mon. Wea. Rev.*, **141**, 3576–3592, doi:10.1175/MWR-D-12-00254.1.

Leroux, M., M. Plu, and F. Roux, 2016: On the sensitivity of tropical cyclone intensification under upper-level trough forcing. *Mon. Wea. Rev.*, **144**, 1179–1202, doi:10.1175/MWR-D-15-0224.1.

Liu, C., and E. A. Barnes, 2015: Extreme moisture transport into the Arctic linked to Rossby wave breaking. *J. Geophys. Res. Atmos.*, **120**, 3774–3788, doi:10.1002/2014JD022796.

Massacand, A. C., H. Wernli, and H. C. Davies, 2001: Influence of upstream diabatic heating upon an alpine event of heavy precipitation. *Mon. Wea. Rev.*, **129**, 2822–2828, doi:10.1175/1520-0493(2001)129<2822:IOUDHU>2.0.CO;2.

McIntyre, M. E., and T. N. Palmer, 1983: Breaking planetary waves in the stratosphere. *Nature*, **305**, 593–600, doi:10.1038/305593a0.

McTaggart-Cowan, R., T. J. Galarneau Jr., L. F. Bosart, R. W. Moore, and O. Martius, 2013: A global climatology of baroclinically influenced tropical cyclogenesis. *Mon. Wea. Rev.*, **141**, 1963–1989, doi:10.1175/MWR-D-12-00186.1.

Michel, C., G. Rivière, L. Terray, and B. Joly, 2012: The dynamical link between surface cyclones, upper-tropospheric Rossby wave breaking and the life cycle of the Scandinavian blocking. *Geophys. Res. Lett.*, **39**, L10806, doi:10.1029/2012GL051682.

Orlanski, I., 2005: A new look at the Pacific storm track variability: Sensitivity to to tropical SSTs and to upstream seeding. *J. Atmos. Sci.*, **62**, 1367–1390, doi:10.1175/JAS3428.1.

Payne, A. E., and G. Magnusdottir, 2014: Dynamics of landfalling atmospheric rivers over the North Pacific in 30 years of MERRA reanalysis. *J. Climate*, **27**, 7133–7150, doi:10.1175/JCLI-D-14-00034.1.

Pokorná, L., and R. Huth, 2015: Climate impacts of the NAO are sensitive to how the NAO is defined. *Theor. Appl. Climatol.*, **119**, 639–652, doi:10.1007/s00704-014-1116-0.

Portis, D. H., J. E. Walsh, M. E. Hamly, and P. J. Lamb, 2001: Seasonality of the North Atlantic Oscillation. *J. Climate*, **14**, 2069–2078, doi:10.1175/1520-0442(2001)014<2069:SOTNAO>2.0.CO;2.

Postel, G. A., and M. H. Hitchman, 1999: A climatology of Rossby wave breaking along the subtropical tropopause. *J. Atmos. Sci.*, **56**, 359–373, doi:10.1175/1520-0469(1999)056<0359:ACORWB>2.0.CO;2.

Rayner, N. A., D. E. Parker, E. B. Horton, C. K. Folland, L. V. Alexander, D. P. Powell, E. C. Kent, and A. Kaplan, 2003: Global analyses of sea surface temperature, sea ice, and night marine air temperature since the late nineteenth century. *J. Geophys. Res.*, **108**, 4407, doi:10.1029/2002JD002670.

Rivière, G., and I. Orlanski, 2007: Characteristics of the Atlantic storm-track eddy activity and its relation with the North Atlantic Oscillation. *J. Atmos. Sci.*, **64**, 241–266, doi:10.1175/JAS3850.1.

Sabbatelli, T. A., and M. E. Mann, 2007: The influence of climate state variables on Atlantic tropical cyclone occurrence rates. *J. Geophys. Res.*, **112**, D17114, doi:10.1029/2007JD008385.

Schneider, T., and S. Bordoni, 2008: Eddy-mediated regime transitions in the seasonal cycle of a Hadley circulation and implications for monsoon dynamics. *J. Atmos. Sci.*, **65**, 915–934, doi:10.1175/2007JAS2415.1.

Strong, C., and G. Magnusdottir, 2008: Tropospheric Rossby wave breaking and the NAO/NAM. *J. Atmos. Sci.*, **65**, 2861–2876, doi:10.1175/2008JAS2632.1.

——, and ——, 2009: The role of tropospheric Rossby wave breaking in the Pacific decadal oscillation. *J. Climate*, **22**, 1819–1833, doi:10.1175/2008JCLI2593.1.

Stuart, A., K. Ord, and S. Arnold, 2009: Partial and multiple correlation. *Classical Inference and the Linear Model*, A. Stuart, K. Ord, and S. Arnold, Eds., Vol. 2A, *Kendall's Advanced Theory of Statistics*, 6th ed. Wiley, 510–537.

Sutton, R. T., and D. L. R. Hodson, 2007: Climate response to basin-scale warming and cooling of the North Atlantic Ocean. *J. Climate*, **20**, 891–907, doi:10.1175/JCLI4038.1.

Thorncroft, C. D., B. J. Hoskins, and M. E. McIntyre, 1993: Two paradigms of baroclinic-wave life-cycle behaviour. *Quart. J. Roy. Meteor. Soc.*, **119**, 17–55, doi:10.1002/qj.49711950903.

Tyrlis, E., and B. J. Hoskins, 2008: The morphology of Northern Hemisphere blocking. *J. Atmos. Sci.*, **65**, 1653–1665, doi:10.1175/2007JAS2338.1.

Vecchi, G. A., and B. J. Soden, 2007: Effect of remote sea surface temperature change on tropical cyclone potential intensity. *Nature*, **450**, 1066–1070, doi:10.1038/nature06423.

——, and G. Villarini, 2014: Next season's hurricanes. *Science*, **343**, 618–619, doi:10.1126/science.1247759.

Villarini, G., G. A. Vecchi, and J. A. Smith, 2010: Modeling the dependence of tropical storm counts in the North Atlantic basin on climate indices. *Mon. Wea. Rev.*, **138**, 2681–2705, doi:10.1175/2010MWR3315.1.

Wang, Y.-H., and G. Magnusdottir, 2011: Tropospheric Rossby wave breaking and the SAM. *J. Climate*, **24**, 2134–2146, doi:10.1175/2010JCLI4009.1.

Waugh, D. W., and L. M. Polvani, 2000: Climatology of intrusions into the tropical upper troposphere. *Geophys. Res. Lett.*, **27**, 3857–3860, doi:10.1029/2000GL012250.

Wentz, F. J., and M. Schabel, 2000: Precise climate monitoring using complementary satellite data sets. *Nature*, **403**, 414–416, doi:10.1038/35000184.

Woollings, T., B. Hoskins, M. Blackburn, and P. Berrisford, 2008: A new Rossby wave-breaking interpretation of the North Atlantic Oscillation. *J. Atmos. Sci.*, **65**, 609–626, doi:10.1175/2007JAS2347.1.

Xie, L., T. Yan, L. J. Pietrafesa, J. M. Morrison, and T. Karl, 2005: Climatology and interannual variability of North Atlantic hurricane tracks. *J. Climate*, **18**, 5370–5381, doi:10.1175/JCLI3560.1.

Zhang, G., and Z. Wang, 2013: Interannual variability of the Atlantic Hadley circulation in boreal summer and its impacts on tropical cyclone activity. *J. Climate*, **26**, 8529–8544, doi:10.1175/JCLI-D-12-00802.1.

——, ——, T. J. Dunkerton, M. S. Peng, and G. Magnusdottir, 2016: Extratropical impacts on Atlantic tropical cyclone activity. *J. Atmos. Sci.*, **73**, 1401–1418, doi:10.1175/JAS-D-15-0154.1.